

## Supplementary Information

### Cobalt Layered Double Hydroxides Nanosheets Synthesized in Water-Methanol Solution as Oxygen Evolution Electrocatalysts

Xiao Xu,<sup>a</sup> Zhou Zhong,<sup>a,b</sup> Xiaomei Yan,<sup>a</sup> Longtian Kang,<sup>a,\*</sup> and Jiannian Yao,<sup>c,\*</sup>

<sup>a</sup> Key Laboratory of Design and Assembly of Functional Nanostructures, and Fujian Provincial Key Laboratory of Nanomaterials, Fujian Institute of Research on the Structure of Matter, Chinese Academy of Sciences, Fuzhou, Fujian 350002, P. R. China.

<sup>b</sup> University of Chinese Academy of Sciences, Chinese Academy of Sciences, Beijing, 100049, P. R. China.

<sup>c</sup> Beijing National Laboratory for Molecular Sciences (BNLMS), Institute of Chemistry, Chinese Academy of Sciences, Beijing 100190, P. R. China.

\*E-mail: longtiank@fjirsm.ac.cn; jnyao@iccas.ac.cn.

## **Supplementary Electrochemical measurements**

A rotating ring-disk electrode (RRDE, PINE Research Instrumentation, 6.5~8.5 mm, 5.5 mm)

was used as the working electrode to test the H<sub>2</sub>O<sub>2</sub> yield. The catalyst loading is 0.084 mg cm<sup>-2</sup>.

The ring potential was set at 0.6 V vs Ag/AgCl. The electron transfer number (n) is calculated from the disk current (J<sub>d</sub>), ring current (J<sub>r</sub>) and current collection efficiency (N=0.38) of the RRDE based on the following Equation.

$$n = \frac{4 \times J_d}{J_r + \frac{J_d}{N}}$$

CV curves were carried out from 0.22 to 0.3 V vs Ag/AgCl to obtain electrochemical double-layer capacitance (C<sub>dl</sub>) by plotting charging current density differences (J<sub>a</sub>-J<sub>c</sub>) at 0.25 V vs Ag/AgCl against scan rates.

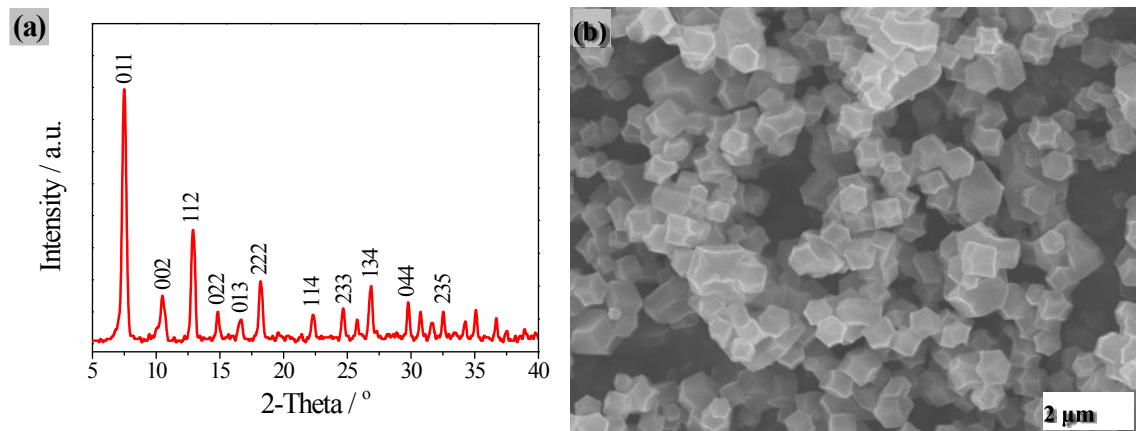


**Fig. S1.** (a) XRD pattern and (b) SEM image of ZIF-67 particles synthesized at 90 °C for 4 h in pure methanol.

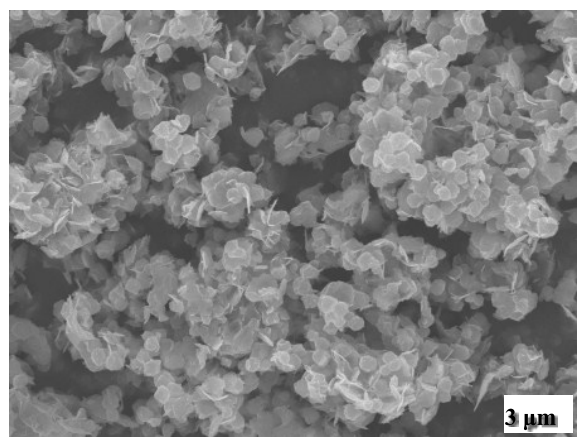


**Fig. S2.** SEM image of composites derived at 90 °C for 4 h in water-methanol solution containing 2 vol% of water.

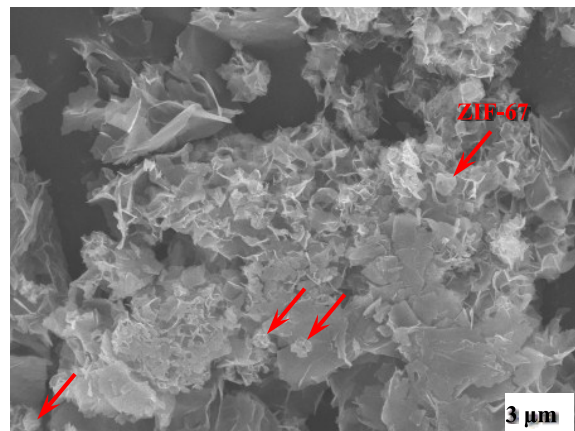


**Fig. S3.** SEM image of composites derived at 90 °C for 4 h in water-methanol solution containing 5 vol% of water.

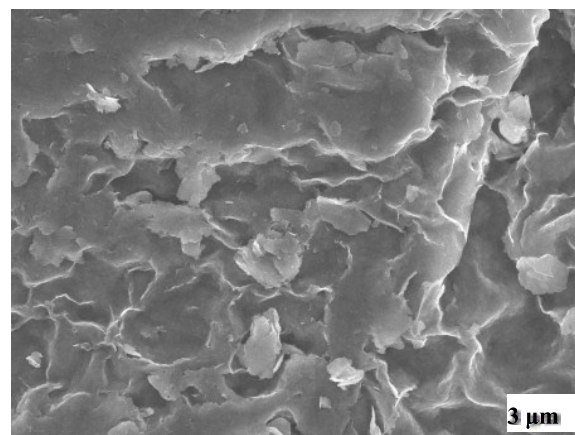


**Fig. S4.** SEM image of composites derived at 90 °C for 4 h in water-methanol solution containing 50 vol% of water.

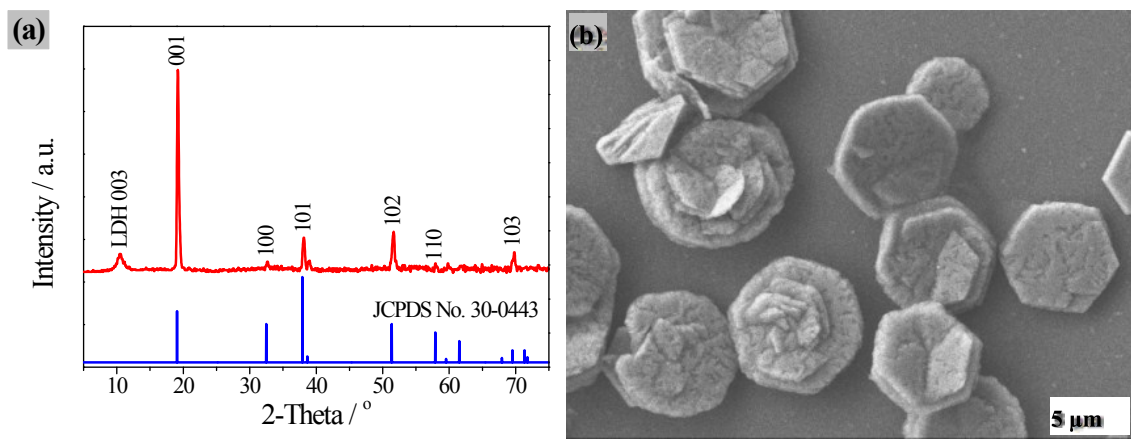


**Fig. S5.** (a) XRD pattern and (b) SEM image of  $\text{Co}(\text{OH})_2$  plates synthesized at 90  $^{\circ}\text{C}$  for 4 h in DI water.

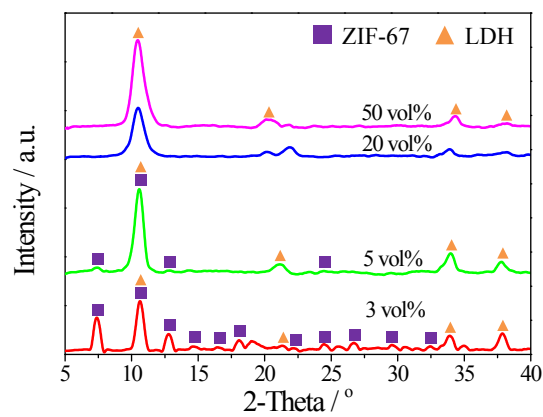


**Fig. S6.** XRD patterns of composites derived at 90  $^{\circ}\text{C}$  for 4 h in water-methanol solution containing different amounts of water.

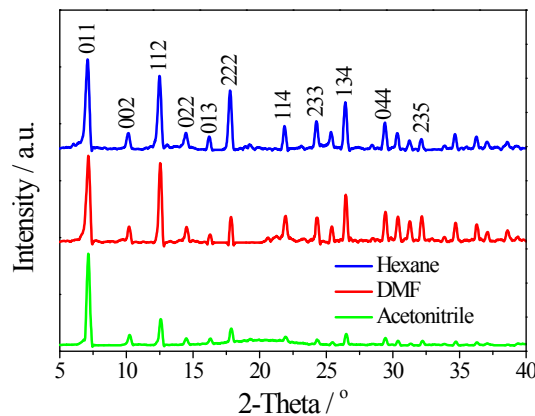


**Fig. S7.** XRD patterns of ZIF-67 particles synthesized at 90 °C for 4 h in methanol solution containing 10 vol% of different solvent: (a) hexane; (b) DMF and (c) acetonitrile.

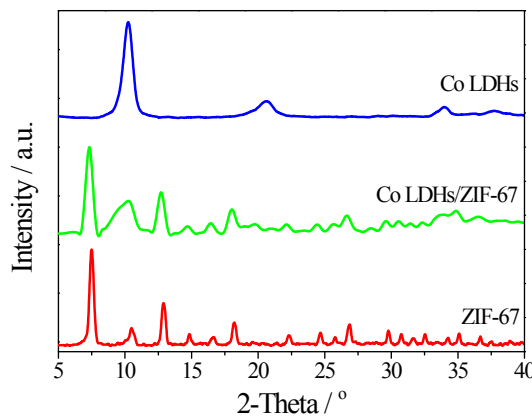


**Fig. S8.** XRD pattern of Co LDHs/ZIF-67 prepared by the hydrolysis reaction of pre-synthesized ZIF-67 (100 mg) at 90 °C for 4 h in water-methanol solution (70 mL) containing 10 vol% of water in the absence of cobalt (II) nitrate.

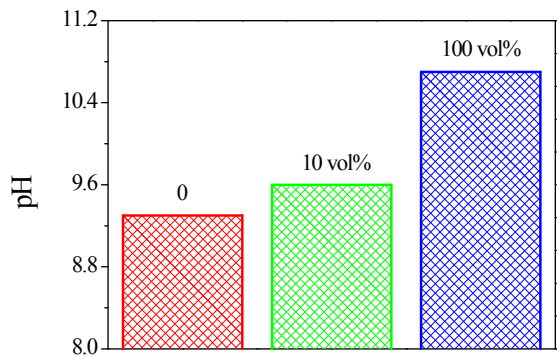


**Fig. S9.** pH value of 2MI (840 mg) in water-methanol solution (70 mL) containing different amounts of water.

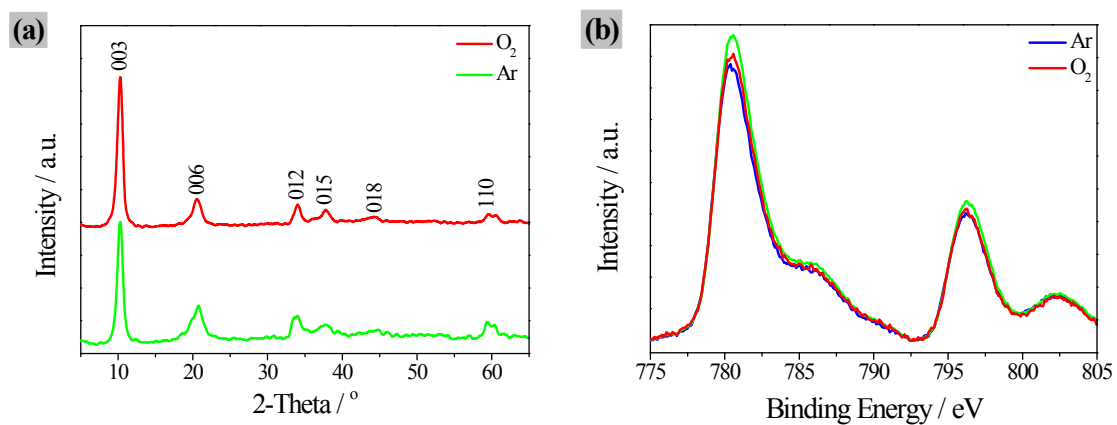


**Fig. S10.** (a) XRD patterns and (b) Co 2p high-resolution XPS spectra for Co LDHs synthesized at 90 °C for 4 h in Ar and O<sub>2</sub>-saturated water-methanol solution containing 10 vol% of water.



**Fig. S11.** Optical images of Co-LDHNS-II: (a) Tyndall effect of colloidal solutions and (b) about 100 mg of dried powders in 5 mL centrifuge tube.

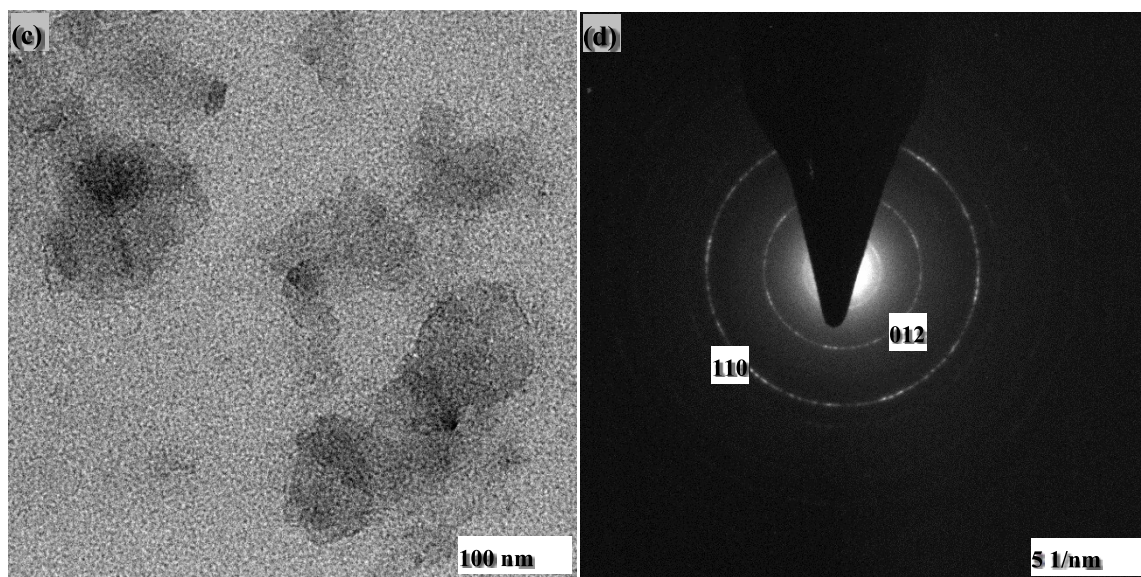


**Fig. S12.** (a) TEM image and (b) selected area diffraction pattern of Co-LDHNS-III.

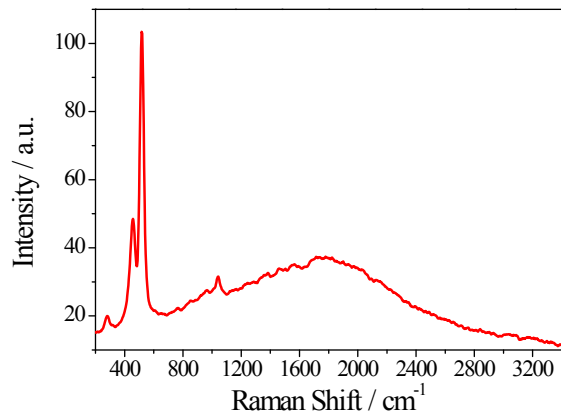


**Fig. S13.** Raman spectrum of Co-LDHNS-II.

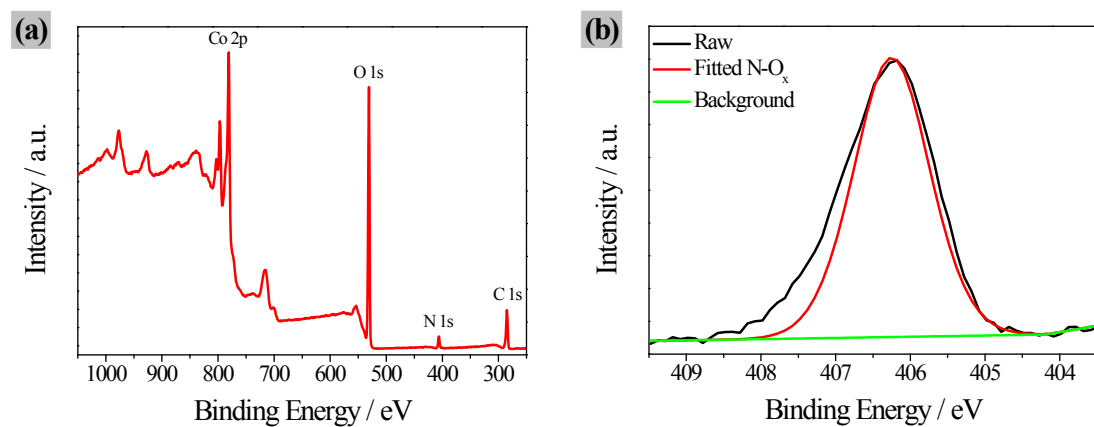


**Fig. S14.** (a) XPS survey spectrum and (b) N 1s high-resolution spectrum of Co-LDHNS-II.

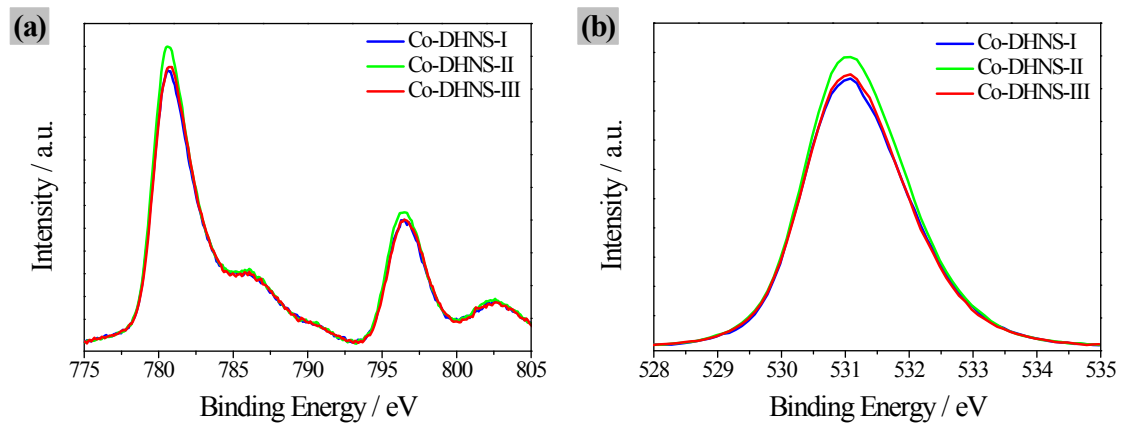


**Fig. S15.** (a) Co 2p and (b) O 1s high-resolution XPS spectra.

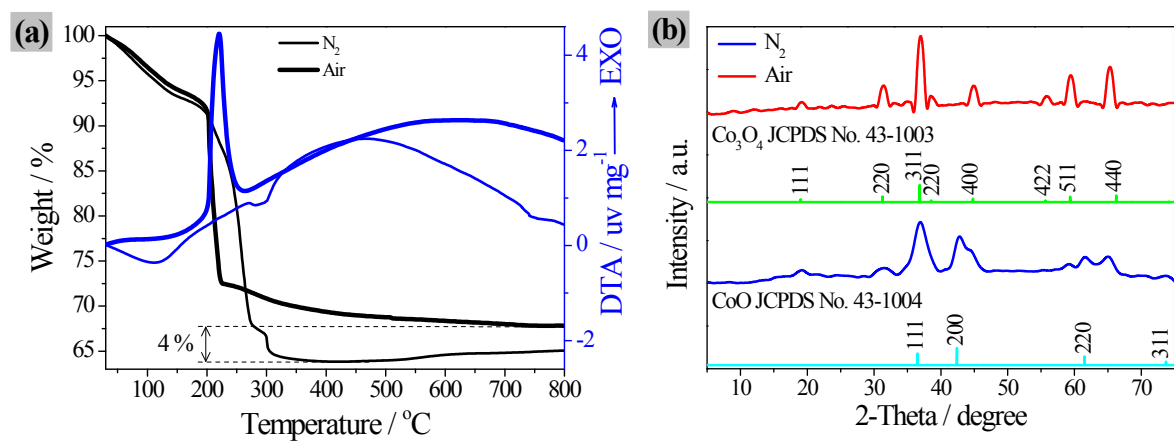


**Fig. S16.** (a) TG-DTA and DSC curves conducted in N<sub>2</sub> and air atmosphere for Co-LDHNS-II and (b) the corresponding XRD patterns after TG measurements.

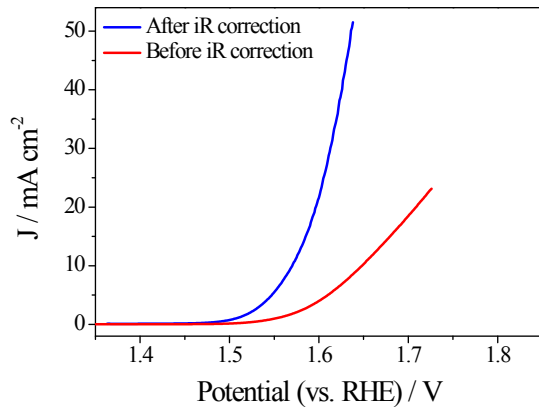


**Fig. S17.** LSV curves of Co-LDHNS-II before and after iR correction at 1600 rpm and  $2 \text{ mV s}^{-1}$  in 1 M KOH.

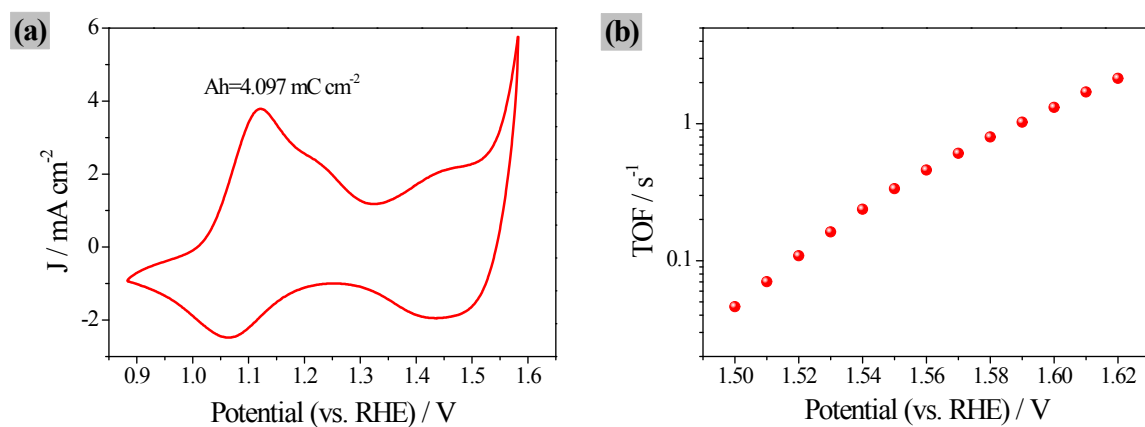


**Fig. S18.** (a) CV curve at  $50 \text{ mV s}^{-1}$  in 1 M KOH and (b) TOF for Co-LDHNS-II.

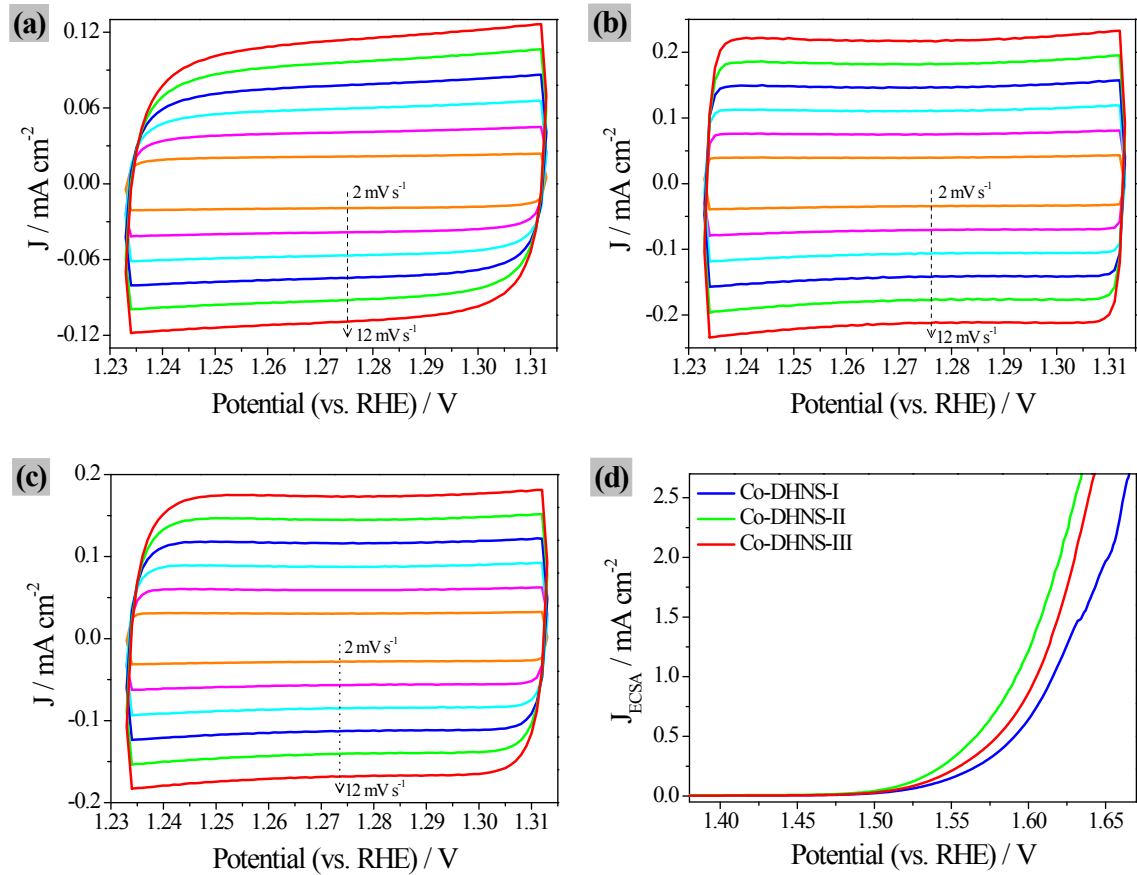


**Fig. S19.** CV curves in the double layer region at 2, 4, 6, 8, 10 and 12  $\text{mV s}^{-1}$  in 1 M KOH for (a) Co-LDHNS-I, (b) Co-LDHNS-II and (c) Co-LDHNS-III. (d) LSV curves normalized by electrochemical surface area (ECSA).

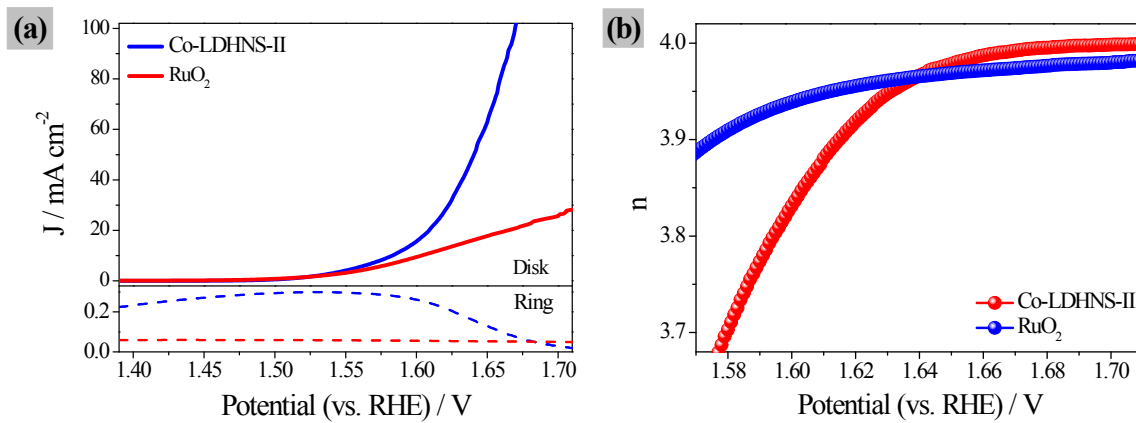


**Fig. S20.** (a) RRDE LSV curves of Co-LDHNS-II and RuO<sub>2</sub> in 1 M KOH. (b) Electron transfer number (n) as a function of applied potentials obtained from (a).

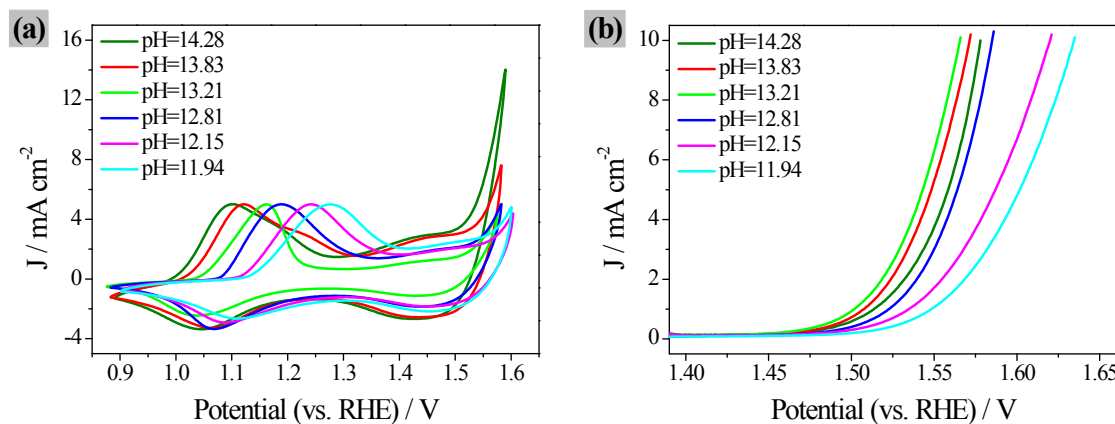


**Fig. S21.** (a) CV curves and (b) LSV curves of Co-LDHNS-II recorded in KOH aqueous solution with varied pH value.

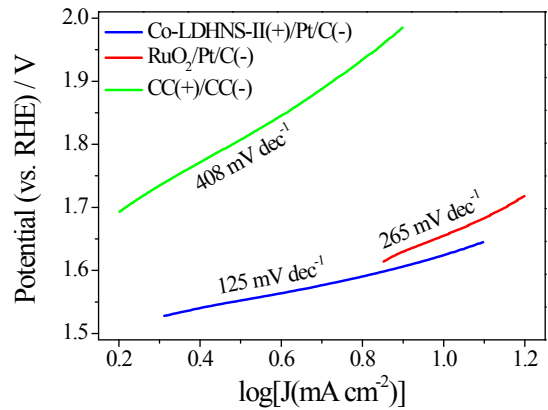


**Fig. S22.** Tafel plots obtained from LSV curves for overall water splitting.

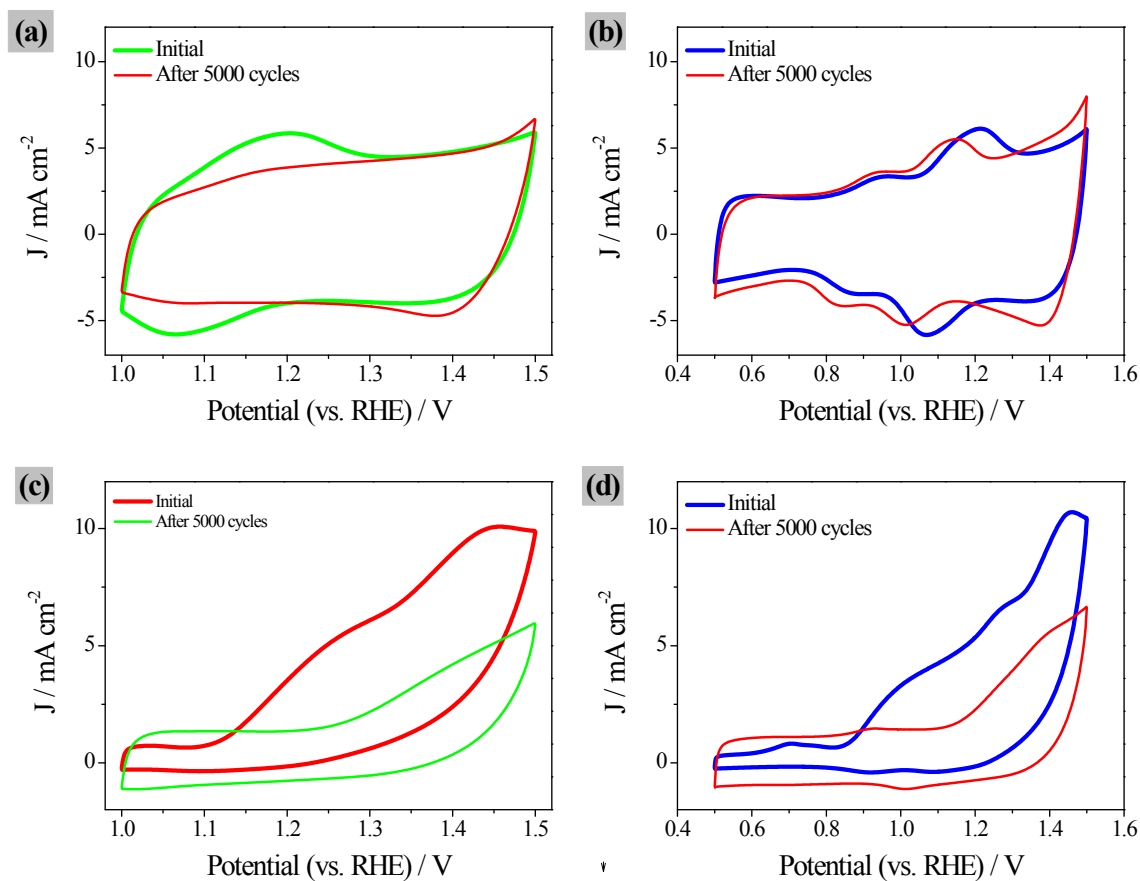


**Fig. S23.** CV curves before and after 5000 cycles: (a, b) Co-LDHNS-II(+)||Pt/C(-) and (c, d)

$\text{RuO}_2(+)\|\text{Pt/C}(-)$ .

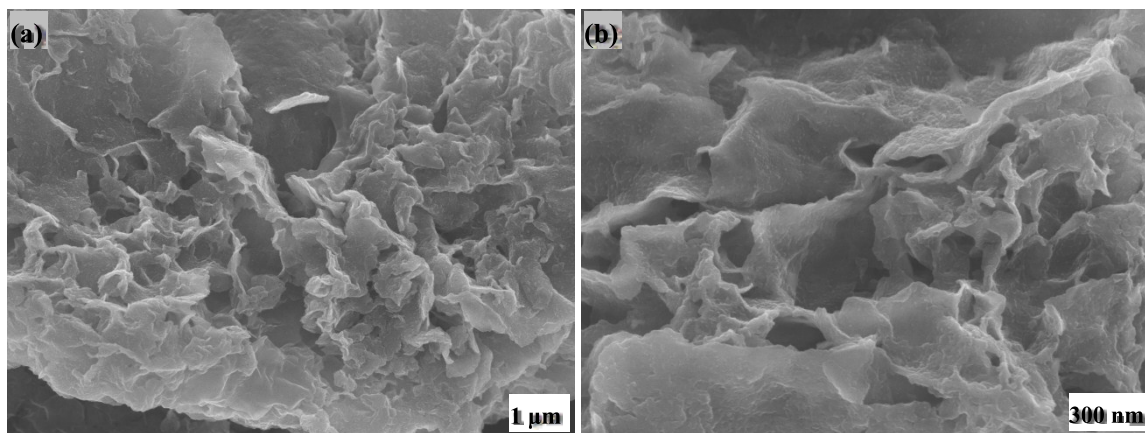


**Fig. S24.** SEM images for Co-LDHNS-II after 5000 cycles of  $\text{Co-LDHNS-II}(+)\|\text{Pt/C}(-)$ .

**Table S1.** Summary of recently reported electrocatalysts for OER.

Electrocatalysts	Substrate	Mass loading [mg cm <sup>-2</sup> ]	Electrolyte	$\eta$ @10 mA cm <sup>-2</sup> [mV]	Tafel slope [mV dec <sup>-1</sup> ]	TOF [s <sup>-1</sup> ]	Ref.
Co-LDHNS-II	GCE	0.1	1 M KOH	340	56	0.801@ $\eta$ =350 mV	This work
	GCE	0.1	0.1 M KOH	356	58	0.262@ $\eta$ =350 mV	
RuO <sub>2</sub>	GCE	0.1	1 M KOH	364	78	/	
Co <sup>2+</sup> @SNG	GCE	/	1 M KOH	370	62	0.266@ $\eta$ =350 mV	S1
CTs/Co-S	CP <sup>c)</sup>	0.32	1 M KOH	306	72	0.016@ $\eta$ =300 mV	S2
CoCo LDH NS <sup>a)</sup>	NF	1	1 M KOH	353	45	0.0035@ $\eta$ =300 mV	S3
NiCo LDH NS	NF	1	1 M KOH	332	40	0.01@ $\eta$ =300 mV	
NCNTFs	GCE	0.2	1 M KOH	370	93	/	S4
20 wt. % Pt/C	GCE	0.2	1 M KOH	550	118	/	
Co-Bi NS/G	GCE	0.285	1 M KOH	290	53	/	S5
RuO <sub>2</sub>	GCE	0.285	1 M KOH	305	60	/	
NiCo LDH NB <sup>b)</sup>	GCE	0.25	1 M KOH	420	135	/	S6
CoFe LDH-Ar	GCE	0.204	1 M KOH	266	38	4.78@ $\eta$ =300 mV	S7
CoFe LDH-F	GCE	0.2	1 M KOH	300	40	/	S8
	NF	1	1 M KOH	260	47	/	
CoAl-NS	3DGN <sup>d)</sup>	0.05±0.01	1 M KOH	252	36	1.14@ $\eta$ =350 mV	S9
IrO <sub>2</sub>	3DGN	0.05±0.01	1 M KOH	277	45	0.73@ $\eta$ =350 mV	
CoMn LDH	GCE	0.142	1 M KOH	324	43	0.13@ $\eta$ =350 mV	S10
IrO <sub>2</sub>	GCE	0.142	1 M KOH	337	49	0.007@ $\eta$ =300 mV	
CoFe LDH NS	CP	0.17	1 M KOH	367	40	/	S11
$\gamma$ -CoOOH NS	GCE	0.15	1 M KOH	300	38	/	S12
CoAl-LDH array	NF	/	1 M KOH	335	128	/	S13
C-Co/Co <sub>3</sub> O <sub>4</sub> HS <sup>e)</sup>	GCE	0.408	1 M KOH	352	80	/	S14
RuO <sub>2</sub>	GCE	0.408	1 M KOH	364	120	/	

<sup>a)</sup>Nanosheets; <sup>b)</sup>Nanoboxes; <sup>c)</sup>Carbon paper; <sup>d)</sup>3D graphene network; <sup>e)</sup>hollow spheres

**Table S2.** Comparison of the water splitting activity of the Co-LDHNS-II with recently reported electrocatalysts in basic solutions.

Electrocatalysts	Substrate	Mass loading [mg cm <sup>-2</sup> ]	Electrolyte	E@10 mA cm <sup>-2</sup>	Tafel slope	Ref.
				[mV]	[mV dec <sup>-1</sup> ]	
Co-LDHNS-II(+)  Pt/C(-)	CC	1	1 M KOH	1.625	125	This work
RuO <sub>2</sub> (+)  Pt/C(-)	CC	1	1 M KOH	1.656	265	
CTs/Co-S(+)  CTs/Co-S(-)	CP	0.32	1 M KOH	1.743	/	S2
RuO <sub>2</sub> (+)  Pt/C(-)	CP	0.32	1 M KOH	1.679	/	
CoFe LDH-F(+)  CoFe LDH-F(-)	NF	1	1 M KOH	1.63	126	S8
IrO <sub>2</sub> (+)  Pt/C(-)	NF	1	1 M KOH	1.63	241	
Pt/C(+)  Pt/C(-)	NF	1	1 M KOH	1.7	206	
VOOH(+)  VOOH(-)	NF	0.8	1 M KOH	1.62	/	S15
RuO <sub>2</sub> (+)  Pt/C(-)	NF	0.8	1 M KOH	1.55	/	
NiFe-MOF(+)  NiFe-MOF(-)	NF	0.3	0.1 M KOH	1.55	256	S16
IrO <sub>2</sub> (+)  Pt/C(-)	NF	/	0.1 M KOH	1.62	267	
CuCoO-NWs(+)  CuCoO-NWs(-)	NF	1.2	1 M KOH	1.61	/	S17
Na <sub>0.08</sub> Ni <sub>0.9</sub> Fe <sub>0.1</sub> O <sub>2</sub> (+)  NiP(-)	NF	0.13	1 M KOH	1.54	/	S18
RuO <sub>2</sub> (+)  Pt/C(-)	NF	0.13	1 M KOH	1.62	/	

## References

- S1 *J. Am. Chem. Soc.*, 2017, **139**, 1878-1884.
- S2 *ACS Nano*, 2016, **10**, 2342-2348.
- S3 *Nat. Commun.*, 2014, **5**, 4477.
- S4 *Nat. Energy*, 2016, **1**, 15006.
- S5 *Angew. Chem. Int. Ed.*, 2016, **55**, 2488-2492.
- S6 *Angew. Chem.*, 2017, **129**, 3955-3958.
- S7 *Angew. Chem.*, 2017, **129**, 5961-5965.
- S8 *ACS Appl. Mater. Interfaces*, 2016, **8**, 34474-34481.
- S9 *Adv. Mater.*, 2016, **28**, 7640-7645.
- S10 *J. Am. Chem. Soc.*, 2014, **136**, 16481-16484.
- S11 *Nano Lett.*, 2015, **15**, 1421-1427.
- S12 *Angew. Chem. Int. Ed.*, 2015, **54**, 8722-8727.
- S13 *Nano Energy*, 2017, **37**, 98-107.
- S14 *J. Mater. Chem. A*, 2017, **5**, 11163-11170.
- S15 *Angew. Chem.*, 2017, **129**, 588-592.
- S16 *Nat. Commun.*, 2017, **8**, 15341.
- S17 *Adv. Funct. Mater.*, 2016, **26**, 8555-8561.
- S18 *Energy Environ. Sci.*, 2017, **10**, 121-128.